Chemistry & Biology
Article

Metabolomics of *Mycobacterium tuberculosis* Reveals Compartmentalized Co-Catabolism of Carbon Substrates

Luiz Pedro S. de Carvalho,[1] Steven M. Fischer,[3] Joeli Marrero,[1] Carl Nathan,[1] Sabine Ehrt,[1] and Kyu Y. Rhee[1,2,*]
[1]Department of Microbiology and Immunology
[2]Division of Infectious Diseases, Department of Medicine
Weill Cornell Medical College, New York, NY 10065, USA
[3]Agilent Technologies, Santa Clara, CA 95051, USA
*Correspondence: kyr9001@med.cornell.edu
DOI 10.1016/j.chembiol.2010.08.009

SUMMARY

Metabolic adaptation to the host environment is a defining feature of the pathogenicity of *Mycobacterium tuberculosis* (Mtb), but we lack biochemical knowledge of its metabolic networks. Many bacteria use catabolite repression as a regulatory mechanism to maximize growth by consuming individual carbon substrates in a preferred sequence and growing with diauxic kinetics. Surprisingly, untargeted metabolite profiling of Mtb growing on ^{13}C-labeled carbon substrates revealed that Mtb could catabolize multiple carbon sources simultaneously to achieve enhanced monophasic growth. Moreover, when co-catabolizing multiple carbon sources, Mtb differentially catabolized each carbon source through the glycolytic, pentose phosphate, and/or tricarboxylic acid pathways to distinct metabolic fates. This unusual topologic organization of bacterial intermediary metabolism has not been previously observed and may subserve the pathogenicity of Mtb.

INTRODUCTION

Mycobacterium tuberculosis (Mtb) is the causative agent of tuberculosis (TB), the leading bacterial cause of deaths worldwide. Among bacterial pathogens, Mtb is unique in that it resides in humans as its only known natural host and reservoir. Mtb has thus evolved to survive within a niche committed to its eradication (Ehrt et al., 2001; Wirth et al., 2008). Prominent among Mtb's adaptations to its singular niche are those pertaining to central carbon metabolism. Transcriptional profiling studies of Mtb recovered from macrophages in vitro and from the lungs of mice and humans demonstrated upregulation of Mtb genes involved in fatty acid catabolism (Bloch and Segal, 1956; Schnappinger et al., 2003; Talaat et al., 2004; Timm et al., 2003). Mtb strains lacking components of the pyruvate dehydrogenase complex, glyoxylate shunt, or the gluconeogenic enzyme phosphoenolpyruvate carboxykinase were defective in replication and attenuated during the chronic phase of infection in a mouse model of pulmonary TB (McKinney et al., 2000; Munoz-Elias and McKinney, 2005; Shi and Ehrt, 2006; Marrero et al., 2010). Carbon metabolism has thus emerged as a major determinant of the pathogenicity of Mtb.

Biochemical knowledge of Mtb carbon metabolism nonetheless remains scant. Genomic and bioinformatic approaches have not cataloged all precursor-product relationships among metabolites. Metabolite levels are similarly often regulated by non-genetic mechanisms, including posttranslational modification and feedback inhibition (Saghatelian and Cravatt, 2005).

Metabolomics is an emerging branch of systems biology that is based on the global and quantitative analysis of low-molecular-weight metabolites in a biological system under a given set of conditions. Metabolomics-based approaches offer integrated readouts of the genome, proteome, and environment on a physiologically global scale (Dettmer et al., 2007; van der Werf et al., 2005; Villas-Boas et al., 2005).

Existing knowledge of carbon metabolism derives heavily from seminal metabolite tracing studies of the model bacterium *Escherichia coli.* These studies taught that different carbon substrates are first catabolized into intermediates of the metabolic pathway closest to their point of entry. Dextrose is thus first catabolized by the glycolytic/gluconeogenic pathway and the pentose phosphate pathway (PPP), whereas glycerol enters the midpoint of the glycolytic/gluconeogenic pathways, and acetate is initially metabolized by the tricarboxylic acid (TCA) cycle. After the first pass through each of these pathways, however, metabolites from each carbon substrate distribute broadly among all 3 pathways to meet the fixed stoichiometric requirements of replication (Herbert et al., 1956; Ingraham et al., 1983). These studies further taught that, when given more than one carbon source, most bacteria consume each carbon source in sequence according to the rate at which each supports growth. That is, most bacteria preferentially consume the carbon source that supports fastest growth until it is depleted and then exhibit a growth lag as they adapt to consume the carbon source supporting next fastest growth (Kovarova-Kovar and Egli, 1998). This phenomenon of diauxic growth is mediated by carbon catabolite repression (CCR), an evolutionarily widespread regulatory trait thought to confer a competitive advantage for a given bacterial species residing within a polymicrobial niche (Gorke and Stulke, 2008).

Mtb, by contrast, dwells chiefly apart from other microbes within the nutritionally stringent environment of the macrophage phagolysosome. Given this unusual niche, we hypothesized that Mtb evolved distinct adaptations of its metabolic network. To test this hypothesis, we undertook a metabolomic analysis of Mtb's central carbon metabolism, focusing on three model carbon substrates, dextrose, acetate, and glycerol. These studies show that Mtb's metabolic topology differs from those described previously in that: (1) Mtb is capable of simultaneously co-catabolizing different carbon sources to augment growth; and (2) this co-catabolism is mediated by the compartmentalized metabolism of each component carbon source to a distinct metabolic fate. To our knowledge, these studies represent the first metabolomic descriptions of Mtb's central carbon metabolism and suggest that Mtb has adapted its metabolic network to maximize growth through the simultaneous co-catabolism of multiple carbon sources.

RESULTS

Mtb Carbon Metabolism during Growth on Dextrose, Acetate, or Glycerol

Early work (Youmans and Youmans, 1953, 1954), recently confirmed (Munoz-Elias and McKinney, 2005), established that Mtb grows fastest in vitro on glycerol, less quickly on dextrose, and least quickly on acetate. These studies however used complex growth media containing additional carbon sources, such as Tween 80, a dispersal agent whose de-esterification can furnish Mb with oleic acid (Dubos and Davis, 1946). We therefore began by studying Mtb's growth and metabolism using defined synthetic media containing equal concentrations of 2-carbon TCA cycle equivalents of dextrose, acetate or glycerol as single carbon sources and replacing Tween 80 with a nonhydrolyzable detergent, Tyloxapol. In aerated batch cultures, Mtb grew fastest and achieved the highest biomass on glycerol, followed by dextrose and acetate (Figure 1; see Figure S1A available online), similar to the earlier studies.

To understand the metabolic basis of Mtb's carbon source-specific growth rate variation, we next sought to define the metabolic fates of each carbon source by global metabolite profiling. Sample preparation presented a key technical hurdle. Detergents used to maintain Mtb in planktonic culture are nonphysiologic; metabolite levels change rapidly during cell collection, such as by centrifugation, and physiologic secretion of metabolites is compounded by leakage as cells are damaged (Brauer et al., 2006; Sani et al., 2010). We overcame these problems by adapting the filter growth method of Brauer et al. (2006). Using chemically defined agar medium, we found that Mtb biomass increased on nitrocellulose filters with slightly slower but comparable kinetics to those in liquid medium of equivalent composition (Figures S1A and S1B). Metabolism of Mtb growing on filters was rapidly quenched by plunging the filters into acetonitrile/methanol/H_2O (40:40:20) precooled to −40°C (Rabinowitz and Kimball, 2007). By using biofilms on filters, we minimized contamination by extracellular fluid. Nonetheless, during thermal quenching, metabolites leaked into the quenching solution (Figure S1C). Therefore, we quenched Mtb in a defined volume, lysed the bacteria mechanically, and analyzed the total pool of metabolites.

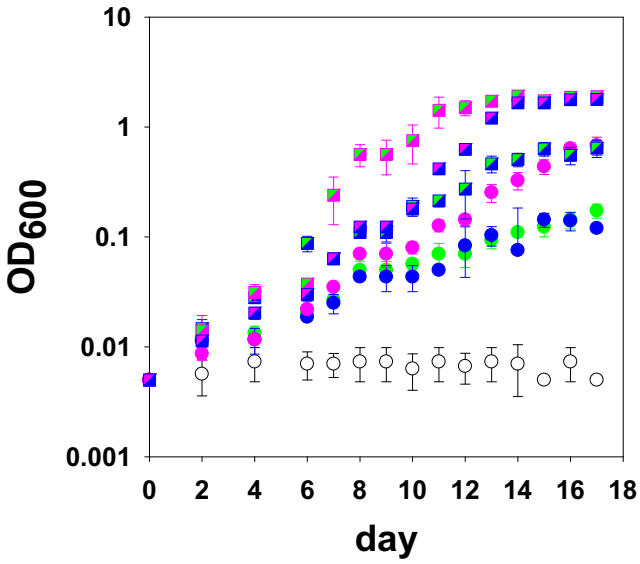

Figure 1. Carbon Source-Specific Variations in Mtb Growth

Mtb growth in liquid media containing no carbon source (open circles), 0.2% (g/100 ml) dextrose (green circles), 0.2% acetate (blue circles), 0.2% glycerol (pink circles), 0.1% dextrose + 0.1% acetate (green- and blue-filled squares), 0.1% dextrose + 0.1% glycerol (green- and pink-filled squares), or 0.1% acetate + 0.1% glycerol (blue- and pink-filled squares). Cells were pregrown on each carbon source or carbon source-mixture for 1 full growth cycle (240 h) or carbon-deprived for the same time and then reinoculated into fresh media of identical chemical composition at 0.02 OD. Growth curves are representative of at least three independent experiments. Error bars represent the standard deviation (SD) of three biological replicates from a single experiment. See also Figure S1.

Metabolites were chromatographed according to chemical class and detected by electrospray ionization-coupled, accurate mass time-of-flight mass spectrometry. This mass spectral scanning approach enabled untargeted indexing and identification of metabolites (defined by co-eluting ion families conforming to discrete empirical formulae) using accurate mass-retention time (AMRT) identifiers. Detected metabolites could then be queried against a pre-populated AMRT library of metabolite standards (Sana et al., 2008). Retention time analysis of known metabolites spanning the chromatographic space demonstrated no significant deviation from those of pure chemical standards (data not shown). For the present study, we focused on primary, water-soluble metabolites, >1000 of which were reproducibly detected by positive and negative mode electrospray ionization.

Using these tools, we traced the specific metabolic fates of uniformly (U) ^{13}C-labeled dextrose, acetate, or glycerol through glycolysis/gluconeogenesis, the pentose phosphate pathway and the TCA cycle. Previous work established that central carbon metabolism operates with quasi-steady state kinetics under logarithmic growth conditions (Hochuli et al., 2000; Sauer et al., 1999; Szyperski et al., 1999). In *E. coli*, half-maximal labeling of most metabolites is achieved within 10–300 s (Yuan et al., 2006). Our preliminary studies with Mtb revealed that isotopic steady state for several key intermediary metabolites was achieved between 6 and 18 h after transfer of filter-laden bacteria taken from the logarithmic phase of growth to fresh ^{13}C-containing medium (Figure S2). We therefore pre-adapted

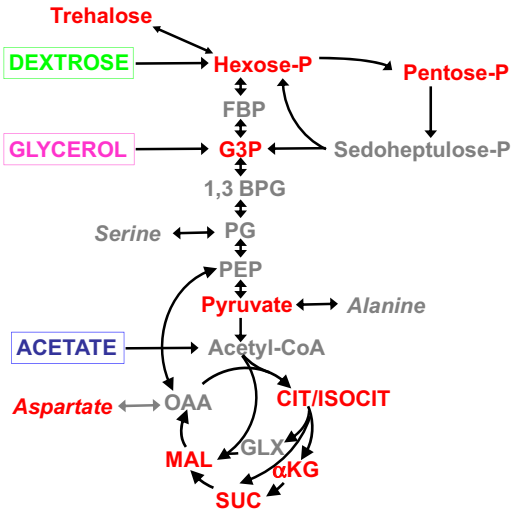

Figure 2. Pathway Diagram of Central Carbon Metabolism

Exemplary metabolite reporters of glycolysis, pentose phosphate pathway and tricarboxylic acid (TCA) cycle used in this study are highlighted in red. Experimental carbon sources used in this study are boxed and their expected entry points into metabolism noted with arrows. In Mtb, the path from α-ketoglutarate to succinate is incompletely defined. αKG: alpha-ketoglutarate, 1,3 BPG: 1,3-bisphosphoglycerate, CIT: citrate, FBP: fructose bisphosphate, G3P: glyceraldehyde phosphate, hexose-P: hexose phosphate, ISOCIT: isocitrate, mal: malic acid, OAA: oxaloacetate, pentose-P: pentose phosphate, PEP: phosphoenolpyruvate, suc: succinic acid, PG: phosphoglycerate.

Mtb to each carbon source or carbon source mixture for nearly one full growth cycle in liquid media, grew them on filters atop chemically equivalent agar media and then transferred to chemically identical media containing a ^{13}C-labeled carbon source for approximately 0.3-generation time (16 h). This allowed us to obtain ^{13}C-labeling patterns representative of both isotopic and metabolic steady state while minimizing uptake of labeled metabolites released by cell turnover. Labeled metabolites were identified by flagging on AMRT species exhibiting nonnatural isotopomeric distributions and analyzing both the ratiometric extent of labeling (as reported by the total isotopomeric proportion of each metabolite pool) and predominant isotopomeric labeling pattern (reflecting the biochemical origin) of each metabolite. For simplicity, we present data for hexose phosphate, glyceraldehyde phosphate, pyruvic acid, pentose phosphate, trehalose, citric/isocitric acid, α-ketoglutaric acid, succinic acid, malic acid, and aspartic acid as exemplary metabolites of these pathways (Figure 2).

As expected, each carbon source was catabolized widely into intermediates of glycolysis/gluconeogenesis, the pentose phosphate pathway and TCA cycle (Figures 3 and 4; Figures S3 and S4) (Munoz-Elias and McKinney, 2006). Growth on U-^{13}C acetate, for example, revealed decreased pool sizes and labeling of α-ketoglutarate. This can be attributed to metabolism of acetate via the glyoxylate shunt (the route from citrate and acetyl CoA to malate and succinate in Figure 2). As also expected we observed increased pool sizes and labeling of intermediates around the metabolic entry point of the parent carbon source during growth on glycerol. Thus, growth on glycerol preferentially enhanced the labeling of glyceraldehyde phosphate (6971 ± 0.1 nmol/mg), the entry point of glycerol, over more metabolically distal intermediates such as hexose phosphate (0.391 ± 0.001 nmol/mg) or pyruvate (from 56 ± 0.01 nmol/mg). Surprisingly, however, growth on dextrose failed to reveal a similar enhancement of the pool size of hexose phosphate (the entry point of dextrose) over more distal intermediates such as glyceryl phosphate or pentose phosphate (Figures 3 and 4; Figures S3 and S4). In addition, nearly all metabolite pool sizes and labeling were greatest for cells growing on glycerol followed by cells growing on dextrose and then cells growing on acetate (Figure 3 and 4; Figures S3 and S4). These results suggest that, during growth on single carbon sources, metabolism of dextrose and acetate is transport-limited (Cook et al., 2009).

Comparisons of growth on either U-^{13}C dextrose or U-^{13}C glycerol further revealed an unexpected dissociation in pool sizes and isotopic labeling between α-ketoglutarate and intermediates of the reductive half of the TCA cycle, succinate, malate, and oxaloacetate (we did not recover oxaloacetate, but inferred its formation from the levels and labeling of aspartic acid, a validated reporter) (Wendisch et al., 2000). This finding thus reveals a significant degree of discontinuity between the two sides of Mtb's TCA cycle.

Mtb Growth and Metabolism during Growth on Carbon Substrate Mixtures

As noted, bacteria given more than one carbon source often exhibit diauxic growth: they consume one carbon source first and their growth curve displays a lag as they adapt to consume the next source (Kovarova-Kovar and Egli, 1998). Early studies, however, reported that Mtb could simultaneously consume dextrose and glycerol without diauxic growth (Bowles and Segal, 1965). We therefore wondered if Mtb could catabolize multiple carbon substrates at once, and if so, whether such co-catabolism would augment growth. To address this question, we studied growth of Mtb on carbon source mixtures in liquid cultures. Growth of a fixed inoculum of Mtb on an equimolar mixture of dextrose and acetate exceeded that achieved with either constituent alone (Figures 1 and 5A Figure S1A). Similar effects were observed using mixtures of dextrose and glycerol and mixtures of acetate and glycerol (Figure 1; Figure S1A). In addition, both Mtb's growth rate and final biomass increased in a dose-dependent manner and with monophasic kinetics when either an increasing amount of dextrose was added to a fixed amount of acetate or an increasing amount of acetate was added to a fixed amount of dextrose (Figures 5B and 5C).

To further address whether Mtb could simultaneously co-catabolize two different carbon sources, we also measured Mtb growth when the ratio of two carbon sources was varied but the total quantity of carbon was held constant. As expected, Mtb growth increased again in proportion to the ratio of dextrose to acetate (Figure 5C). Sequential utilization of carbon sources in mixtures predicts that the maximum achievable growth rate is that corresponding to the carbon source supporting fastest growth. This model further predicts that the final biomass achieved roughly equals the sum of the biomass of each of the sub-populations growing on a single carbon source. Neither of these results pertained for Mtb. Instead, Mtb grew with monophasic kinetics at a growth rate greater than that observed on an equimolar amount of each component alone and achieved

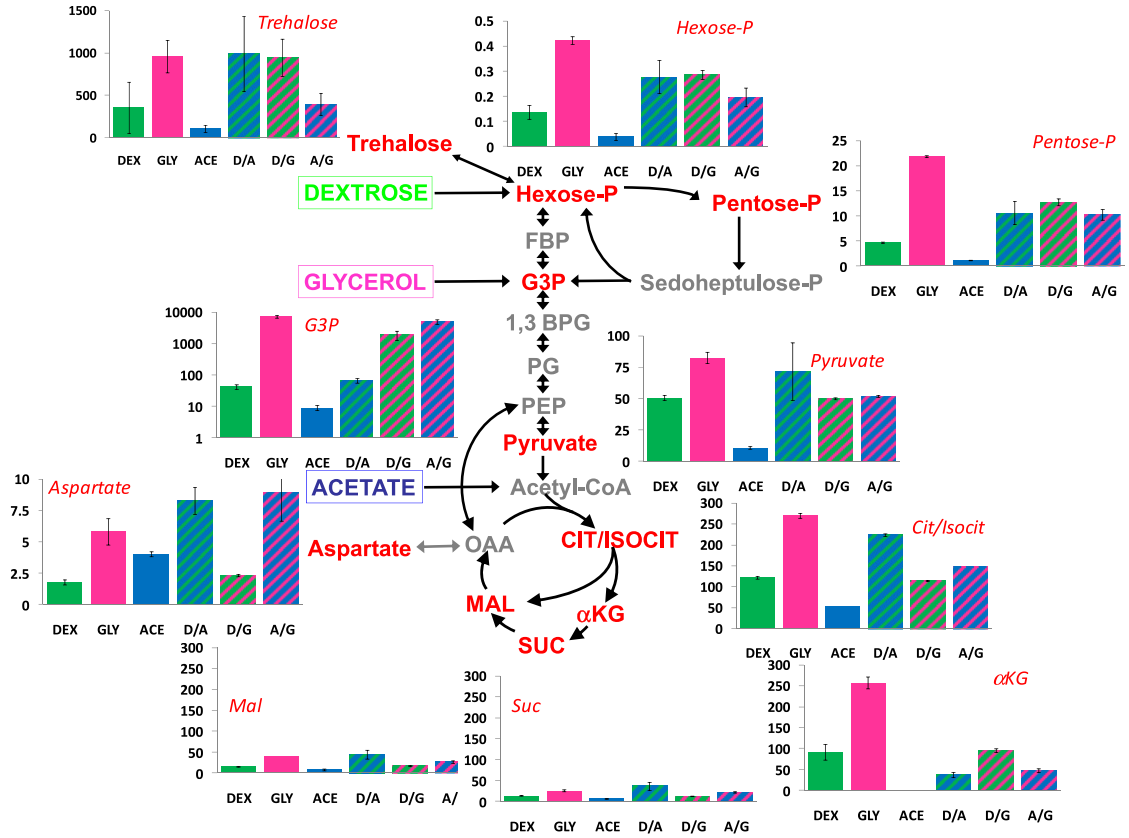

Figure 3. Metabolite Pool Sizes in Mtb during Logarithmic Growth on Dextrose, Acetate, and/or Glycerol

Carbon sources are indicated on the x axis. Pool sizes expressed as nmol/mg protein are indicated on the y axis on individually different linear scales, or in the case of glyceraldehyde-3-phosphate, on a logarithmic scale. Individual carbon sources were provided at 0.2% for studies of single carbon sources and at 0.1% for studies of carbon source mixtures, so that there were equivalent concentrations of 2-carbon units in all cases. Color scheme corresponds to those used in Figures 1 and 2. Error bars represent the SD of biological replicates (n = 3). ACE: acetate, A/G: acetate/glycerol, αKG: alpha-ketoglutarate, 1,3 BPG: 1,3-bisphosphoglycerate, CIT: citrate, D/A: dextrose/acetate, DEX: dextrose, D/G: dextrose/glycerol, FBP: fructose bisphosphate, GLY: glycerol, G3P: glyceraldehyde phosphate, hexose-P: hexose phosphate, ISOCIT: isocitrate, mal: malic acid, OAA: oxaloacetate, pentose-P: pentose phosphate, PEP: phosphoenolpyruvate, suc: succinic acid, PG: phosphoglycerate. See also Figure S3.

a final biomass greater than the predicted sum of biomasses achieved on each component alone (Figure 1 and Figure 5). These results thus establish Mtb's ability to simultaneously catabolize two different carbon sources and regulate growth in response to both the total quantity and composition of carbon sources encountered.

Given these findings, we traced the specific metabolic fates of dextrose, acetate, and glycerol during growth on the same carbon source mixtures. To do so, we pre-adapted Mtb to the carbon mixture of interest, grew them on filters to the logarithmic phase and then transferred to equivalent media containing one U-^{13}C-labeled and one unlabeled carbon source for 16 h, a time at which isotopic steady state had been achieved. These studies (Figures 3 and 4; Figures S3 and S4) revealed incorporation of ^{13}C from each carbon source into metabolites of glycolysis/gluconeogenesis, the pentose phosphate pathway and TCA cycle. The additive contributions of each carbon substrate to growth (Figures 1 and 5) excluded the possibility that these results reflected the activity of two noninteracting bacterial subpopulations, each of which catabolized a single carbon source. These results thus confirm Mtb's ability to simultaneously co-catabolize two different carbon sources and lack of catabolite repression among the three carbon sources examined.

Like growth, metabolite pool sizes varied with both the number and identities of carbon sources supplied (Figure 3; Figure S3). However, metabolite pool sizes exhibited no strict correlation with the identity or quantity of any single carbon source or with the specific composition of any individual carbon source mixture. For example, during growth on an equimolar mixture of 0.1% dextrose and 0.1% acetate, pool sizes of many, though not all, metabolites examined were significantly greater than those associated with growth on either 0.2% dextrose or 0.2% acetate alone or those predicted from the additive metabolism of 0.1% of each (Figure S3) (e.g., compare hexose phosphate pool sizes during growth on 0.1% dextrose + 0.1% acetate [277 ± 66 pmol/mg] versus growth on 0.2% dextrose [136 ± 28 pmol/mg] or 0.2% acetate alone [39 ± 14 pmol/mg]). In contrast, metabolite pool sizes associated with carbon mixtures containing 0.1% glycerol were uniformly equal to or smaller than those achieved on 0.2% glycerol alone, and corresponded most closely to pool sizes predicted by the

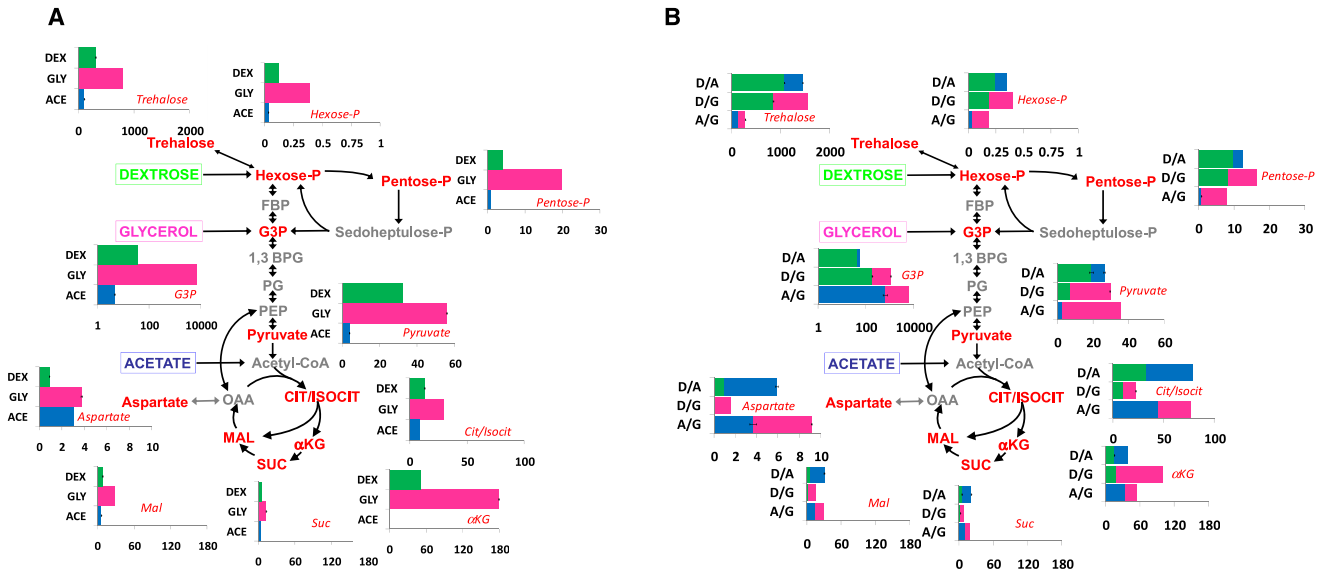

Figure 4. Metabolic Distribution of U-^{13}C Isotopic-Labeled Dextrose, Acetate and/or Glycerol in Mtb After Uptake

Stacked bar plots demonstrating isotopic incorporation of U-^{13}C carbon source into the intracellular pool of selected metabolites. Carbon sources are indicated on the y axis. Isotopic labeling is indicated on the x axis as nmol labeled/mg protein/16 h labeling interval on individually different linear scales, or in the case of glyceraldehyde-3-phosphate, on a logarithmic scale. Individual carbon sources were provided at 0.2% for studies of single carbon sources and at 0.1% for studies of carbon source mixtures, so that there were equivalent concentrations of 2-carbon units in all cases. For carbon source mixtures, the extent of isotopic labeling achieved by each component carbon source is represented by the length of the corresponding colored segment. On the logarithmic scale for glyceraldehyde-3-phosphate, short segments at the right of the scale can denote a far higher extent of labeling than long segments at the left of the scale. Calculations were corrected for signals arising from naturally occurring isotopomeric species associated with the unlabeled metabolite pool. Symbols and color scheme are as in Figure 3. Error bars represent the standard deviation of biological replicates (n = 3). See also Figure S4.

additive metabolism of 0.1% of each (Figure S3). Growth on all glycerol-containing mixtures nonetheless equaled or exceeded that achieved with glycerol alone. These results thus revealed major metabolic adaptations associated with growth on mixed carbon sources.

Isotopic labeling analysis further revealed that, during growth on carbon source mixtures, Mtb metabolized each component carbon source to a distinct metabolic fate (Figure 4; Figure S4). For example, during growth on an equimolar mixture of dextrose and acetate, Mtb preferentially metabolized dextrose into glycolytic and pentose phosphate pathway intermediates while directing acetate into intermediates of the TCA cycle. These preferences were reflected by differences in the extent of metabolic labeling associated with each carbon source when metabolized alone and when co-metabolized with a second carbon source. Growth on an equimolar mixture of 0.1% dextrose and 0.1% acetate, for example, revealed an increased labeling of hexose phosphate (246 ± 0.6 pmol/mg) from U-^{13}C dextrose compared to that derived from U-^{13}C acetate (100 ± 1 pmol/mg) and that observed during growth on 0.2% U-^{13}C

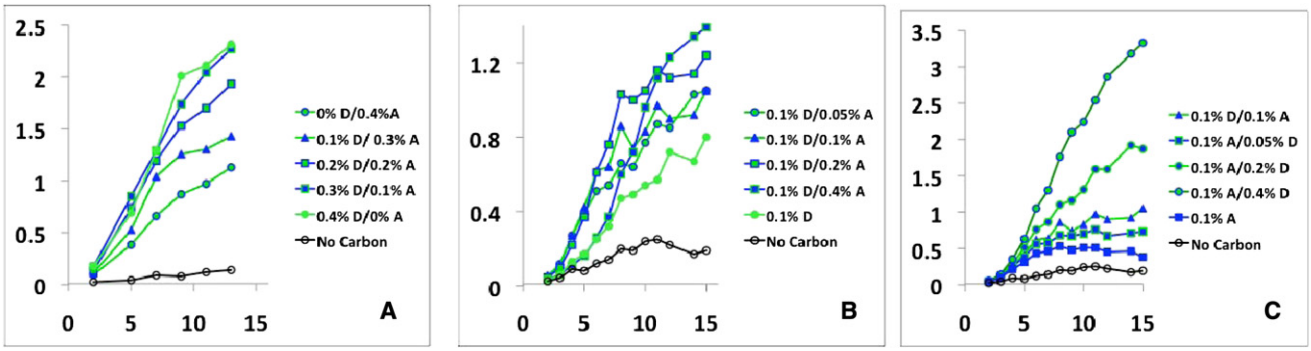

Figure 5. Composition-Specific Variation of Mtb Growth on Carbon Source Mixtures

Mtb growth was followed by measuring the optical density of liquid cultures containing no carbon or carbon source mixtures with: (A) a fixed amount of dextrose and increasing amounts of acetate; (B) a fixed amount of acetate and increasing amounts of dextrose; or (C) a fixed total carbon content (0.4%) and varying ratios of dextrose (D) and acetate (A) as indicated. Growth curves are representative of three replicate experiments. Error bars represent the standard deviation of biological replicates (n = 3).

dextrose alone (33 ± 0.1 pmol/mg). Growth on an equimolar mixture of 0.1% U-^{13}C acetate and 0.1% unlabeled dextrose similarly revealed an increased labeling of malate from U-^{13}C acetate (25 ± 0.74 nmol/mg) compared to that derived from U-^{13}C dextrose (5.47 ± 0.18 nmol/mg) and that observed during growth on 0.2% U-^{13}C acetate alone (6.0 ± 0.08 nmol/mg).

These findings were independently confirmed by isotopomeric profiling analysis of each labeled metabolite. That is, when U-^{13}C acetate was co-metabolized with dextrose, the ^{13}C was less extensively incorporated into higher order isotopomers of hexose phosphate than when acetate was metabolized alone. This shift reflects an increased flux of (and isotopic dilution with) carbon derived from metabolism of unlabeled dextrose and relative decrease in acetate-derived ^{13}C flux (Figure S5). Conversely, incorporation of dextrose-derived ^{13}C into malate decreased when co-metabolized with acetate.

Glycerol, by contrast, exhibited a fixed metabolic fate. As previously noted, metabolism of glycerol gave rise to metabolite pool sizes corresponding to those predicted by the additive metabolism of 0.1% glycerol with either 0.1% dextrose or 0.1% acetate. Catabolism of 0.1% U-^{13}C glycerol with either dextrose or acetate similarly gave rise to ^{13}C labeling levels ~50% of that achieved during growth on 0.2% U-^{13}C glycerol alone (Figure 4; Figure S4). Glycerol metabolism was thus unaffected by the presence of a second carbon source.

Glycerol metabolism nonetheless enhanced catabolism of U-^{13}C dextrose or U-^{13}C acetate to the same compartmentalized fates as those observed when dextrose and acetate were co-catabolized with one another (Figure 4; Figure S4). For example, co-catabolism with glycerol enhanced metabolism of U-^{13}C dextrose into hexose phosphate (0.186 ± 0.001 nmol/mg) over that observed during metabolism of twice as much U-^{13}C dextrose alone (0.122 ± 0.001 nmol/mg). Co-catabolism with glycerol similarly increased metabolism of U-^{13}C acetate into malate (15.7 ± 0.1 nmol/mg) over that observed during metabolism of twice as much U-^{13}C acetate alone (6.02 ± 0.08 nmol/mg). Thus, co-catabolism of glycerol with U-^{13}C dextrose enhanced labeling of intermediates early in glycolysis and the pentose phosphate shunt whereas co-catabolism of glycerol with U-^{13}C acetate enhanced labeling of TCA cycle intermediates (Figure 4; Figure S4).

The foregoing studies revealed that Mtb could simultaneously co-catabolize different carbon sources to distinct metabolic fates. However, these studies also revealed that this compartmentalization was incomplete. That is, while co-catabolizing dextrose and acetate, Mtb preferentially metabolized dextrose into intermediates of glycolysis and the pentose phosphate pathway, but preferentially used acetate for TCA cycle intermediates. However, at the same time, Mtb also incorporated low levels of acetate-derived ^{13}C into glycolytic/gluconeogenic and pentose phosphate intermediates (Figure 4; Figure S4). The same phenomenon was also observed during growth on mixtures of dextrose and glycerol (Figure 4; Figure S4). These findings thus demonstrate that Mtb is not only capable of co-catabolizing different carbon sources to compartmentalized fates but can also direct simultaneous flux of each carbon source through the same metabolic pathways but in opposite directions, such as the case for glycolysis and gluconeogenesis.

DISCUSSION

In this sudy, we have used the term ''compartmentalization'' to refer to the predominant use of different carbon sources to feed different pathways (Figure 6). However, as noted above, some pathways operated bidirectionally, albeit asymmetrically, such as simultaneous glycolysis and gluconeogenesis. Surprisingly, when given both dextrose and acetate, Mtb used carbon from dextrose for glycolysis, but still maintained low level carbon flow from acetate through gluconeogenesis. This functional separation was maintained at steady state. We will use the term ''segregation'' to describe sustained functional separation in the sources of carbon that sustain flux in different directions on the same pathway. Operation of compartmentalization and segregation indicates that Mtb has evolved a highly modular metabolic network capable of adapting to the number and identities of carbons sources available.

Bacteria face the challenge of coordinating thousands of biochemical reactions, many of which are mutually competitive, in an ostensibly homogeneous space. Existing knowledge of bacterial carbon metabolism derives heavily from microbes that exhibit diauxic growth (Kovarova-Kovar and Egli, 1998). In these species, this challenge has been met, in part, through the widespread regulatory phenomenon of carbon catabolite repression (CCR). CCR is a complex and mechanistically diverse phenomenon by which cells specifically adapt metabolism to the carbon source that supports fastest growth. In *Enterobacteriaceae* and Firmicutes, this has been achieved through the action of a conserved phosphoenolpyruvate: carbohydrate phosphotransferase system (PTS) that coordinately regulates carbohydrate transport and expression of genes involved in carbon catabolism. In *Actinobacteria* however, which include mycobacteria, an increasing number of diverse PTS-independent CCR mechanisms have been reported. Notwithstanding, this trait gives rise to the sequential pattern of carbon utilization manifest as diauxic growth and is believed to confer a competitive advantage over other microbes residing in the same ecologic niche (Gorke and Stulke, 2008).

For many bacteria, however, carbon is encountered only in quantities and forms that, alone, are insufficient for significant growth. It is likely therefore that such organisms have evolved metabolic regulatory mechanisms apart from CCR. Mtb's unique ecological niche suggests the need for such alternative mechanisms. Within the host, Mtb resides chiefly within the macrophage phagolysosome, a nutritionally stringent environment devoid of other microbes, where it is commonly thought to persist in a slow or non-replicating state for the lifetime of the host (Barry et al., 2009; Gill et al., 2009; Schnappinger et al., 2003). Over the natural course of its life-cycle, however, Mtb also encounters brief largesse of carbon such as in the necrotic tissue and caseum of one host and the lymph and blood of a newly infected one (Esteban et al., 2001; Fitzgerald et al., 2009; McDonald et al., 1999; von Gottberg et al., 2001). Thus, although it remains possible that Mtb may operate catabolite repression under conditions not tested herein, Mtb must still regulate metabolism to persist within the nutritionally stringent host phagolysosome and remain poised to replicate at a rate sufficient to infect, but not prematurely kill, a new host. It is plausible therefore that Mtb has evolved a modular metabolic

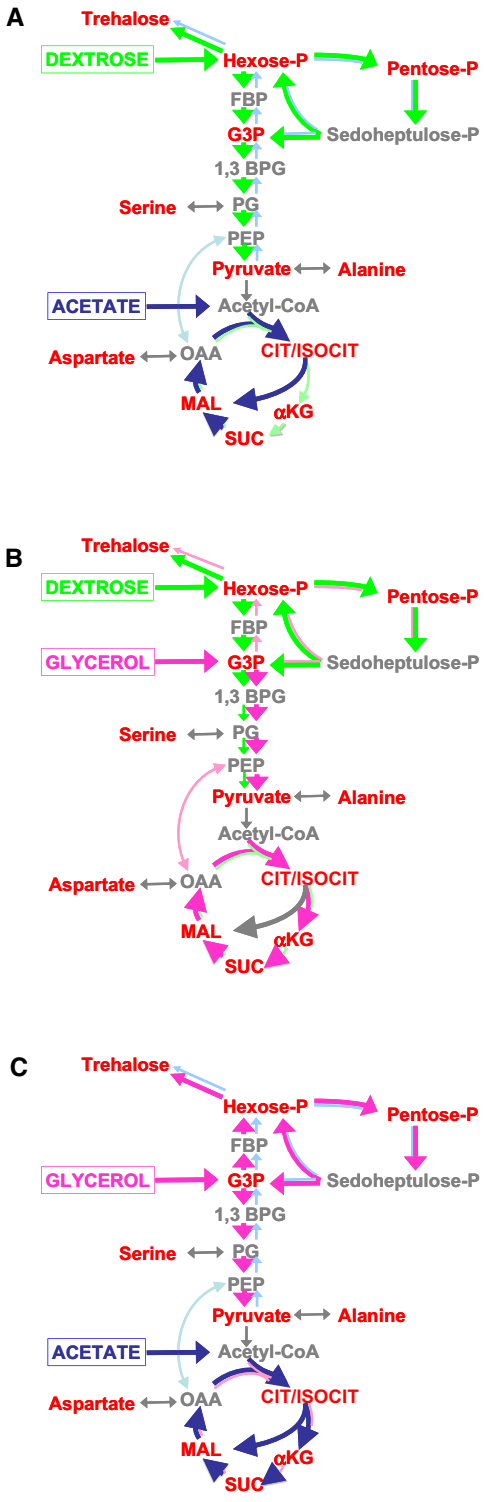

Figure 6. Metabolic Pathway Diagram of Central Carbon Metabolism in Mtb

Pathway schematic of glycolysis/gluconeogenesis, pentose phosphate shunt, and TCA cycle indicating distinct metabolic fates of dextrose (green), acetate (blue), and glycerol (pink) during growth on carbon substrate mixtures of: (A) dextrose and acetate, (B) dextrose and glycerol, and (C) acetate and glycerol (based on data shown in Figures 2 and 3). Exemplary metabolite reporters of glycolysis, pentose phosphate pathway, and TCA cycle are highlighted in red. The color and thickness of the arrows connecting metabolites indicates the predominant pattern of distribution of the corresponding carbon source. Abbreviations are as in legend to Figure 2.

network. Although this may seem inefficient from a bioenergetic perspective, it may, in fact, be essential for propagation of a pathogen with an ultra-narrow host range.

Carbon co-catabolism has previously been reported among heterotrophic bacteria. However, such studies largely reported co-consumption or depletion of metabolically homologous carbon sources (for example, two sugars) with little to no knowledge of their specific metabolic fates (Kovarova-Kovar and Egli, 1998). Among Actinobacteria, only *Corynebacterium glutamicum* has been reported to co-catabolize heterologous carbon sources, where it was found that dextrose and acetate were catabolized to highly overlapping metabolic fates (Wendisch et al., 2000). Kleijn et al. (2010) similarly reported co-catabolism of dextrose and malate in the firmicute *Bacillus subtilis*, but observed compartmentalized metabolism of each carbon source primarily during growth on single carbon sources, where it was chiefly localized around the metabolic entry point of the carbon source used. Mtb is thus unprecedented in its ability to simultaneously channel different carbon sources to separate, and complementary, metabolic fates. Moreover, although we can not exclude the possibility of CCR in Mtb with other carbon sources, we believe that Mtb is the first bacterial pathogen found to lack classical catabolite (dextrose) repression and regulate growth through simultaneous co-catabolism of multiple carbon sources.

Early studies suggested that Mtb could simultaneously consume multiple carbon sources during batch growth in vitro (Bowles and Segal, 1965). Genome sequencing efforts later revealed that Mtb lacked identifiable orthologs to the core PTS system associated with canonical (dextrose-induced) catabolite repression mechanisms (Cole et al., 1998). Biochemical knowledge of Mtb carbon metabolism, however, remained scant.

Our discovery of Mtb's capacity to simultaneously co-catabolize multiple carbon sources suggests that Mtb may have specifically evolved to optimize intracellular carbon flux across a diverse range of environmental conditions. This view is affirmed by the fact that the overall metabolite pool sizes and carbon fluxes achieved during growth on mixed carbon sources did not strictly conform to those predicted by the additive metabolism of each component carbon source alone. Additional evidence for such adaptation includes the apparent lack of feedback inhibition by the glycolytic intermediate, fructose 1,6 bisphosphate, on Mtb's glycerol kinase, as revealed by Mtb's ability to simultaneously co-catabolize dextrose and glycerol (Zwaig and Lin, 1966). Together, such findings may help explain Mtb's metabolic adaptability and raise the intriguing possibility that Mtb's survival may not be tied to the availability of any single carbon source.

It remains to be determined how Mtb segregates metabolism of individual carbon sources from one another during co-catabolism and achieves their compartmentalized metabolic fates. However, the following speculations may serve as a guide. Growing evidence indicates that enzymes of a given module of intermediary metabolism may reversibly form multiprotein

complexes in response to the nutritional environment of the cell and its physiological needs (An et al., 2008; Fan et al., 2010; Narayanaswamy et al., 2009; Savage et al., 2010; Tanaka et al., 2010). Such complexes may facilitate more efficient channeling of substrates and products through these pathways. More recent work has demonstrated that, on a global scale, enzymes often subserve multiple functions related to bacterial metabolism (Yus et al., 2009). Alternatively, it is possible that the recently described outer membrane of Mtb may create a metabolically competent periplasmic space housing one or more modules of intermediary metabolism, whereas others reside in the cytosol (An et al., 2008; Hoffmann et al., 2008; Kuhner et al., 2009; Sani et al., 2010; Zuber et al., 2008). Such physical compartmentalization would be analogous to the situation in eukaryotic cells that localize different modules of intermediary metabolism in the cytosol and mitochondrial matrix. In this regard, it is especially interesting to consider whether the fixed metabolic fate of glycerol may reflect the ability of glycerol to passively diffuse across lipid membranes whereas dextrose and acetate require active transport mechanisms, perhaps into physically separate compartments (Cook et al., 2009).

The present work greatly expands the database of pool sizes of metabolites in Mtb's central carbon metabolism (Tian et al., 2005a). This new information raises many questions for further exploration. For example, the evident discontinuity between the pool sizes and carbon flux of the oxidative and reductive branches of the TCA cycle (Figure 3) suggests that the lack of α-ketoglutarate dehydrogenase in Mtb is not fully compensated by the recently described aerotolerant anaerobic type α-ketoglutarate ferredoxin-oxidoreductase (Baughn et al., 2009; Tian et al., 2005b). Indeed, the directionality of carbon flow through Mtb's TCA cycle during aerobic growth remains unresolved. Additional key aspects of Mtb's central metabolic pathways thus await further study.

Overall, we believe these studies provide the first biochemical descriptions of Mtb's metabolic network at the level of its metabolites and suggest that this network has an unprecedented structure. Mtb's metabolic network topology may contribute to Mtb's pathogenicity. Future metabolite tracing studies promise to reveal additional key aspects of Mtb metabolism not accessible by existing genomic or proteomic approaches.

SIGNIFICANCE

Carbon metabolism in most bacteria is subject to catabolite repression, a widespread regulatory trait by which bacteria maximize growth by consuming individual carbon substrates in a preferred sequence, and exhibit a diauxic pattern of growth. We show that Mtb, the causative agent of TB, does not exhibit diauxic growth and can, in fact, catabolize multiple carbon sources simultaneously, leading to enhanced monophasic growth. Moreover, we show that during co-catabolism, Mtb catabolizes each carbon source differentially through the glycolytic, pentose phosphate and/or tricarboxylic acid pathways to distinct metabolic fates. This ability to simultaneously channel carbohydrates and fatty acids to distinct metabolic fates represents a previously undescribed metabolic network topology among bacteria and reshapes our basic understanding of Mtb's capacity to adapt to the host niche. This work illustrates the potential of metabolomics to deliver knowledge not accessible by existing genomic, proteomic, biochemical or bioinformatic approaches: in this case, the first evidence of metabolic compartmentalization in a cell lacking organelles.

EXPERIMENTAL PROCEDURES

Bacterial Strains and Cultivation

Mtb strain H37Rv was cultivated in 7H9 liquid medium supplemented with 0.5 g/l Fraction V bovine serum albumin, 0.05% Tyloxapol, and dextrose, acetate, and/or glycerol. For metabolomic profiling studies, Mtb was cultivated on 7H10 agar supplemented with 0.5 g/l Fraction V bovine serum albumin, 0.05% Tyloxapol, and dextrose, acetate, and/or glycerol according to Brauer et al. (2006) (Bradford, 1976). Mtb was thus first grown in 7H9 liquid media containing the carbon source(s) of interest until the late logarithmic phase and then inoculated onto 22 mm 0.22 μm nitrocellulose filters under vacuum filtration. Mtb-laden filters were then placed atop chemically equivalent agar media (described above) and allowed to grow at 37°C. Bacterial growth was monitored by sacrificing replicate Mtb-laden filters and following cell wet weights, which increased with constant doubling times from ~day 3 through day 8. Mtb-laden filters were transferred on day 5 to chemically identical ^{13}C-containing agar media to allow isotopic labeling of metabolites. Bacteria were metabolically quenched by plunging Mtb-laden filters into acetonitrile/methanol/H_2O (40:40:20) precooled to −40°C and metabolites extracted by mechanically lysing the entire Mtb-containing solution with 0.1 mm Zirconia beads in a Precellys tissue homogenizer for 8 min under continuous cooling at or below 2°C. Lysates were clarified by centrifugation and then filtered across a 0.22 μm filter. Bacterial biomass of individual samples was determined by measuring the residual protein content of metabolite extracts.

Liquid Chromatography-Mass Spectrometry

Metabolites were separated on a Cogent Diamond Hydride Type C column as detailed by Pesek et al. (2008) (Gradient 3). The mobile phase consisted of the following: solvent A (water containing 0.2% acetic acid) and solvent B (acetonitrile containing 0.2% acetic acid). The gradient used was as follows: 0–2 min, 85% B; 3–5 min, 80% B; 6–7 min, 75%; 8–9 min, 70% B; 10–11.1 min, 50% B; 11.1–14 min 20% B; 14.1–24 min 5% B followed by a 10 min re-equilibration period at 85% B at a flow rate of 0.4 ml/min. The mass spectrometer used was an Agilent Accurate Mass 6220 TOF coupled to an Agilent 1200 LC system. Dynamic mass axis calibration was achieved by continuous infusion of a reference mass solution using an isocratic pump with a 100:1 splitter. This configuration achieved mass errors of ~5 ppm, mass resolution ranging from 10,000 to 25,000 (over m/z 121–955 AMU), and 5 $\log_{10}$ dynamic range. Detected ions were deemed metabolites on the basis of unique accurate mass-retention time identifiers for masses exhibiting the expected distribution of accompanying isotopomers. Metabolite identities were searched for using a mass tolerance of <0.005 Da. Metabolites were quantified using a calibration curve generated with chemical standard spiked into homologous mycobacterial extract to correct for matrix-associated ion suppression effects.

Isotopomer Data Analysis

The extent of isotopic labeling for each metabolite was determined by dividing the summed peak height ion intensities of all labeled species by the ion intensity of both labeled and unlabeled species, expressed in percent. Label-specific ion counts were corrected for naturally occurring ^{13}C species (i.e., [M+1] and [M+2]). The relative abundance of each isotopically labeled species was determined by dividing the peak height ion intensity of each isotopic form (corrected for naturally occurring ^{13}C species as above) by the summed peak height ion intensity of all labeled species.

SUPPLEMENTAL INFORMATION

Supplemental Information includes five figures and can be found with this article online at doi:10.1016/j.chembiol.2010.08.009.

ACKNOWLEDGMENTS

We thank Tiffany Butterfield for technical support and Steven Gross and Qiuying Chen for discussions. This work was supported by the Burroughs Wellcome Career Award in the Biomedical Sciences, the Bill and Melinda Gates Foundation, and the William Randolph Hearst Foundation (KYR). The Department of Microbiology & Immunology acknowledges the support of the William Randolph Hearst Foundation.

Received: March 5, 2010
Revised: July 26, 2010
Accepted: August 20, 2010
Published: October 28, 2010

REFERENCES

An, S., Kumar, R., Sheets, E.D., and Benkovic, S.J. (2008). Reversible compartmentalization of de novo purine biosynthetic complexes in living cells. Science *320*, 103–106.

Barry, C.E., 3rd, Boshoff, H.I., Dartois, V., Dick, T., Ehrt, S., Flynn, J., Schnappinger, D., Wilkinson, R.J., and Young, D. (2009). The spectrum of latent tuberculosis: rethinking the biology and intervention strategies. Nat. Rev. Microbiol. *7*, 845–855.

Baughn, A.D., Garforth, S.J., Vilcheze, C., and Jacobs, W.R., Jr. (2009). An anaerobic-type alpha-ketoglutarate ferredoxin oxidoreductase completes the oxidative tricarboxylic acid cycle of *Mycobacterium tuberculosis*. PLoS Pathog. *5*, e1000662.

Bloch, H., and Segal, W. (1956). Biochemical differentiation of *Mycobacterium tuberculosis* grown in vivo and in vitro. J. Bacteriol. *72*, 132–141.

Bowles, J.A., and Segal, W. (1965). Kinetics of utilization of organic compounds in the growth of *Mycobacterium tuberculosis*. J. Bacteriol. *90*, 157–163.

Bradford, M.M. (1976). A rapid and sensitive method for the quantitation of microgram quantities of protein utilizing the principle of protein-dye binding. Anal. Biochem. *72*, 248–254.

Brauer, M.J., Yuan, J., Bennett, B.D., Lu, W., Kimball, E., Botstein, D., and Rabinowitz, J.D. (2006). Conservation of the metabolomic response to starvation across two divergent microbes. Proc. Natl. Acad. Sci. USA *103*, 19302–19307.

Cole, S.T., Brosch, R., Parkhill, J., Garnier, T., Churcher, C., Harris, D., Gordon, S.V., Eiglmeier, K., Gas, S., Barry, C.E., 3rd., et al. (1998). Deciphering the biology of *Mycobacterium tuberculosis* from the complete genome sequence. Nature *393*, 537–544.

Cook, G.M., Berney, M., Gebhard, S., Heinemann, M., Cox, R.A., Danilchanka, O., and Niederweis, M. (2009). Physiology of mycobacteria. Adv. Microb. Physiol. *55*, 81–182, 318–189.

Dettmer, K., Aronov, P.A., and Hammock, B.D. (2007). Mass spectrometry-based metabolomics. Mass Spectrom. Rev. *26*, 51–78.

Dubos, R.J., and Davis, B.D. (1946). Factors affecting the growth of tubercle bacilli in liquid media. J. Exp. Med. *83*, 409–423.

Ehrt, S., Schnappinger, D., Bekiranov, S., Drenkow, J., Shi, S., Gingeras, T.R., Gaasterland, T., Schoolnik, G., and Nathan, C. (2001). Reprogramming of the macrophage transcriptome in response to interferon-gamma and *Mycobacterium tuberculosis*: signaling roles of nitric oxide synthase-2 and phagocyte oxidase. J. Exp. Med. *194*, 1123–1140.

Esteban, J., de Gorgolas, M., Santos-O'Connor, F., Gadea, I., Fernandez-Roblas, R., and Soriano, F. (2001). *Mycobacterium tuberculosis* bacteremia in a university hospital. Int. J. Tuberc. Lung Dis. *5*, 763–768.

Fan, C., Cheng, S., Liu, Y., Escobar, C.M., Crowley, C.S., Jefferson, R.E., Yeates, T.O., and Bobik, T.A. (2010). Short N-terminal sequences package proteins into bacterial microcompartments. Proc. Natl. Acad. Sci. USA *107*, 7509–7514.

Fitzgerald, D.W., Sterling, T.R., and Haas, D.W. (2009). Mycobacterium tuberculosis. In Principles and Practice of Infectious Diseases, G.L. Mandell, J.E. Bennett, and R. Dolin, eds. (Philadelphia: Churchill Livingstone).

Gill, W.P., Harik, N.S., Whiddon, M.R., Liao, R.P., Mittler, J.E., and Sherman, D.R. (2009). A replication clock for *Mycobacterium tuberculosis*. Nat. Med. *15*, 211–214.

Gorke, B., and Stulke, J. (2008). Carbon catabolite repression in bacteria: many ways to make the most out of nutrients. Nat. Rev. Microbiol. *6*, 613–624.

Herbert, D., Elsworth, R., and Telling, R.C. (1956). The continuous culture of bacteria; a theoretical and experimental study. J. Gen. Microbiol. *14*, 601–622.

Hochuli, M., Szyperski, T., and Wuthrich, K. (2000). Deuterium isotope effects on the central carbon metabolism of *Escherichia coli* cells grown on a D_2O-containing minimal medium. J. Biomol. NMR *17*, 33–42.

Hoffmann, C., Leis, A., Niederweis, M., Plitzko, J.M., and Engelhardt, H. (2008). Disclosure of the mycobacterial outer membrane: cryo-electron tomography and vitreous sections reveal the lipid bilayer structure. Proc. Natl. Acad. Sci. USA *105*, 3963–3967.

Ingraham, J.L., Maaloe, O., and Neidhardt, F. (1983). Growth of the Bacterial Cell (Sunderland: Sinauer).

Kleijn, R.J., Buescher, J.M., Le Chat, L., Jules, M., Aymerich, S., and Sauer, U. (2010). Metabolic fluxes during strong carbon catabolite repression by malate in *Bacillus subtilis*. J. Biol. Chem. *285*, 1587–1596.

Kovarova-Kovar, K., and Egli, T. (1998). Growth kinetics of suspended microbial cells: from single-substrate-controlled growth to mixed-substrate kinetics. Microbiol. Mol. Biol. Rev. *62*, 646–666.

Kuhner, S., van Noort, V., Betts, M.J., Leo-Macias, A., Batisse, C., Rode, M., Yamada, T., Maier, T., Bader, S., Beltran-Alvarez, P., et al. (2009). Proteome organization in a genome-reduced bacterium. Science *326*, 1235–1240.

Marrero, J., Rhee, K.Y., Schnappinger, D., Pethe, K., and Ehrt, S. (2010). Gluconeogenic carbon flow of tricarboxylic acid cycle intermediates is critical for *Mycobacterium tuberculosis* to establish and maintain infection. Proc. Natl. Acad. Sci. USA *107*, 9819–9824.

McDonald, L.C., Archibald, L.K., Rheanpumikankit, S., Tansuphaswadikul, S., Eampokalap, B., Nwanyanawu, O., Kazembe, P., Dobbie, H., Reller, L.B., and Jarvis, W.R. (1999). Unrecognized *Mycobacterium tuberculosis* bacteriemia among hospital inpatients in less developed countries. Lancet *354*, 1159–1163.

McKinney, J.D., Honer zu Bentrup, K., Munoz-Elias, E.J., Miczak, A., Chen, B., Chan, W.T., Swenson, D., Sacchettini, J.C., Jacobs, W.R., Jr., and Russell, D.G. (2000). Persistence of *Mycobacterium tuberculosis* in macrophages and mice requires the glyoxylate shunt enzyme isocitrate lyase. Nature *406*, 735–738.

Munoz-Elias, E.J., and McKinney, J.D. (2005). *Mycobacterium tuberculosis* isocitrate lyases 1 and 2 are jointly required for in vivo growth and virulence. Nat. Med. *11*, 638–644.

Munoz-Elias, E.J., and McKinney, J.D. (2006). Carbon metabolism of intracellular bacteria. Cell. Microbiol. *8*, 10–22.

Narayanaswamy, R., Levy, M., Tsechansky, M., Stovall, G.M., O'Connell, J.D., Mirrielees, J., Ellington, A.D., and Marcotte, E.M. (2009). Widespread reorganization of metabolic enzymes into reversible assemblies upon nutrient starvation. Proc. Natl. Acad. Sci. USA *106*, 10147–10152.

Pesek, J.J., Matyska, M.T., Fischer, S.M., and Sana, T.R. (2008). Analysis of hydrophilic metabolites by high-performance liquid chromatography-mass spectrometry using a silica hydride-based stationary phase. J. Chromatogr. A *1204*, 48–55.

Rabinowitz, J.D., and Kimball, E. (2007). Acidic acetonitrile for cellular metabolome extraction from Escherichia coli. Anal. Chem. *79*, 6167–6173.

Saghatelian, A., and Cravatt, B.F. (2005). Global strategies to integrate the proteome and metabolome. Curr. Opin. Chem. Biol. *9*, 62–68.

Sana, T.R., Roark, J.C., Li, X., Waddell, K., and Fischer, S.M. (2008). Molecular formula and METLIN Personal Metabolite Database matching applied to the identification of compounds generated by LC/TOF-MS. J. Biomol. Tech. *19*, 258–266.

Sani, M., Houben, E.N., Geurtsen, J., Pierson, J., de Punder, K., van Zon, M., Wever, B., Piersma, S.R., Jimenez, C.R., Daffe, M., et al. (2010). Direct visualization by cryo-EM of the mycobacterial capsular layer: a labile structure containing ESX-1-secreted proteins. PLoS Pathog. *6*, e1000794.

Sauer, U., Lasko, D.R., Fiaux, J., Hochuli, M., Glaser, R., Szyperski, T., Wuthrich, K., and Bailey, J.E. (1999). Metabolic flux ratio analysis of genetic and environmental modulations of *Escherichia coli* central carbon metabolism. J. Bacteriol. *181*, 6679–6688.

Savage, D.F., Afonso, B., Chen, A.H., and Silver, P.A. (2010). Spatially ordered dynamics of the bacterial carbon fixation machinery. Science *327*, 1258–1261.

Schnappinger, D., Ehrt, S., Voskuil, M.I., Liu, Y., Mangan, J.A., Monahan, I.M., Dolganov, G., Efron, B., Butcher, P.D., Nathan, C., et al. (2003). Transcriptional adaptation of *Mycobacterium tuberculosis* within macrophages: insights into the phagosomal environment. J. Exp. Med. *198*, 693–704.

Shi, S., and Ehrt, S. (2006). Dihydrolipoamide acyltransferase is critical for *Mycobacterium tuberculosis* pathogenesis. Infect. Immun. *74*, 56–63.

Szyperski, T., Glaser, R.W., Hochuli, M., Fiaux, J., Sauer, U., Bailey, J.E., and Wuthrich, K. (1999). Bioreaction network topology and metabolic flux ratio analysis by biosynthetic fractional 13C labeling and two-dimensional NMR spectroscopy. Metab. Eng. *1*, 189–197.

Talaat, A.M., Lyons, R., Howard, S.T., and Johnston, S.A. (2004). The temporal expression profile of *Mycobacterium tuberculosis* infection in mice. Proc. Natl. Acad. Sci. USA *101*, 4602–4607.

Tanaka, S., Sawaya, M.R., and Yeates, T.O. (2010). Structure and mechanisms of a protein-based organelle in Escherichia coli. Science *327*, 81–84.

Tian, J., Bryk, R., Itoh, M., Suematsu, M., and Nathan, C. (2005a). Variant tricarboxylic acid cycle in *Mycobacterium tuberculosis*: identification of alpha-ketoglutarate decarboxylase. Proc. Natl. Acad. Sci. USA *102*, 10670–10675.

Tian, J., Bryk, R., Shi, S., Erdjument-Bromage, H., Tempst, P., and Nathan, C. (2005b). *Mycobacterium tuberculosis* appears to lack alpha-ketoglutarate dehydrogenase and encodes pyruvate dehydrogenase in widely separated genes. Mol. Microbiol. *57*, 859–868.

Timm, J., Post, F.A., Bekker, L.G., Walther, G.B., Wainwright, H.C., Manganelli, R., Chan, W.T., Tsenova, L., Gold, B., Smith, I., et al. (2003). Differential expression of iron-, carbon-, and oxygen-responsive mycobacterial genes in the lungs of chronically infected mice and tuberculosis patients. Proc. Natl. Acad. Sci. USA *100*, 14321–14326.

van der Werf, M.J., Jellema, R.H., and Hankemeier, T. (2005). Microbial metabolomics: replacing trial-and-error by the unbiased selection and ranking of targets. J. Ind. Microbiol. Biotechnol. *32*, 234–252.

Villas-Boas, S.G., Mas, S., Akesson, M., Smedsgaard, J., and Nielsen, J. (2005). Mass spectrometry in metabolome analysis. Mass Spectrom. Rev. *24*, 613–646.

von Gottberg, A., Sacks, L., Machala, S., and Blumberg, L. (2001). Utility of blood cultures and incidence of mycobacteremia in patients with suspected tuberculosis in a South African infectious disease referral hospital. Int. J. Tuberc. Lung Dis. *5*, 80–86.

Wendisch, V.F., de Graaf, A.A., Sahm, H., and Eikmanns, B.J. (2000). Quantitative determination of metabolic fluxes during co-utilization of two carbon sources: comparative analyses with *Corynebacterium glutamicum* during growth on acetate and/or glucose. J. Bacteriol. *182*, 3088–3096.

Wirth, T., Hildebrand, F., Allix-Beguec, C., Wolbeling, F., Kubica, T., Kremer, K., van Soolingen, D., Rusch-Gerdes, S., Locht, C., Brisse, S., et al. (2008). Origin, spread and demography of the *Mycobacterium tuberculosis* complex. PLoS Pathog. *4*, e1000160.

Youmans, A.S., and Youmans, G.P. (1954). Studies on the metabolism of *Mycobacterium tuberculosis*. IV. The effect of fatty acids on the growth of *M. tuberculosis* var. *hominis*. J. Bacteriol. *67*, 731–733.

Youmans, G.P., and Youmans, A.S. (1953). Studies on the metabolism of *Mycobacterium tuberculosis*. I. The effect of carbohydrates and alcohols on the growth of *Mycobacterium tuberculosis var. hominis*. J. Bacteriol. *65*, 92–95.

Yuan, J., Fowler, W.U., Kimball, E., Lu, W., and Rabinowitz, J.D. (2006). Kinetic flux profiling of nitrogen assimilation in *Escherichia coli*. Nat. Chem. Biol. *2*, 529–530.

Yus, E., Maier, T., Michalodimitrakis, K., van Noort, V., Yamada, T., Chen, W.H., Wodke, J.A., Guell, M., Martinez, S., Bourgeois, R., et al. (2009). Impact of genome reduction on bacterial metabolism and its regulation. Science *326*, 1263–1268.

Zuber, B., Chami, M., Houssin, C., Dubochet, J., Griffiths, G., and Daffe, M. (2008). Direct visualization of the outer membrane of mycobacteria and corynebacteria in their native state. J. Bacteriol. *190*, 5672–5680.

Zwaig, N., and Lin, E.C. (1966). Feedback inhibition of glycerol kinase, a catabolic enzyme in *Escherichia coli*. Science *153*, 755–757.